UNIVERSITY OF Southampton

Design Journal Summary
FEEG6013 Group Design Project

25
VENAS
Veneer Assessment System

ID Number: 31145914
Name: Tan Yee Jie

Primary Supervisor: Dr. Richard Cook

Co-Supervisors: Meisam Jalavand

Submitted on: 09/05/2024

1. Summary of individual contribution

The VENAS project aimed to achieve a design that can identifies "deflects" on a piece of wood veneer in a data driven way. Deflects are mostly quantifies as stress concentration point, as those are the region that would fails under the forming process of our stakeholder. As illustrated in ***Figure 1 - 1***, I am assigned as the design and manufacture team in this project. My main role consists of helping the team in achieving stakeholder's requirements by designing and selecting the optimal solutions that fulfills the requirements. It is also my responsibility to manufacture relevant part for prototyping.

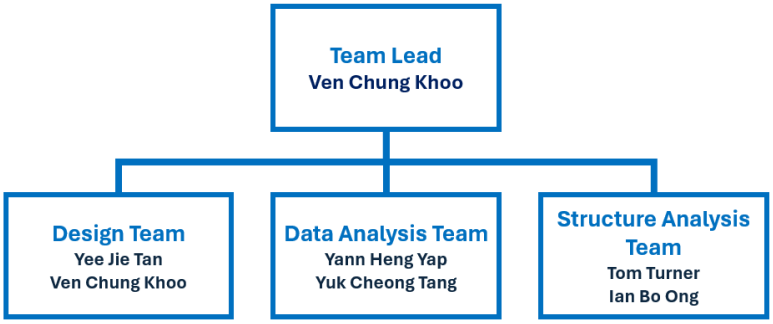

Figure 1 - 1: Team Structure Overview.

Throughout the project, the final design proposal has been split into smaller sub-sections for local design and search. As the team established that sophisticated experiments and investigations must be conducted to identify the features on the veneer that depicted concerned, my part as the design team in the early stage is to acquire pieces of information through available apparatus. This helps in determining the specifications needed for the designs, and crucially also the helps wood structure team, in conducting more thorough experiments based off early acquired information. However, with my main roles being the design team, the focus on my work on the later stages are mostly design, search, and optimizations.

2. Roles, activities, and outputs

2.1 Initial Designs

In the earlier stages, the information including appearance of the veneer are unsure. The initial concept designs illustrated in journal entry 1 are thus, aimed to identify stress concentration points based of available, common criteria online. The scanning method, from literature past work, concludes into laser scattering method [3], air-coupled ultrasonic method [2], and acoustical wave measurements [1]. As evident in journal entry 1, the common stress concentration points such as knots are usually visible by naked eyes, hence I proposed to include camera as a choice for the scanning method. The literature found scanning module are mostly density-based, or structural-based methods, camera that provides an appearance visualization can be combined with another method to provide even thorough search on the veneer, hence this explains for the combinations between distinct scanning module in the initial sketches.

After concluding everyone's initial sketches, a relatively systematic method is needed to evaluate the choices. Hence, the weighted matrix is created by the Ven and me, to not only investigated the

viability of each choice effectively, but also documenting the process for future revisits. ***Table 2.1 - 1*** demonstrated one of the key weighted matrices, which helps us in making the decision of either moving scanning module (fixed platform) or a moving platform (fixed scanning module). Note that the matrix is updated several times after the first attempt, after receiving feedback upon, hence the table shown might differ from journal entry 1. As the scoreline of the moving scanning module is higher, it will be chosen as the optimal design option to proceed with.

Evaluation Criteria	Moving Scanner Module	Fixed Scanner Module
Spatial Resolution	0	0
Power usage	0	0
Ease of Manufacturing	0	1
Ease of Maintenance	0	1
Affordability	-1	0
Durability of System	0	1
Versatility for Veneer Size	1	-1
Novelty	0	-1
Safety	0	1
Reliability	0	-1
TOTAL	**1**	**0**

Table 2.1 - 1 : Weighting Matrix of Fixed or Moving Scanning Module:

Notably, a conceptual, or idea design is created based on the chosen option of enabling motion on the scanning module, to provide an insight towards our future design.

2.2 Initial Investigation

2.2.1 C-T and Microscopy

C-T scan is one of the available options to investigate in the early stages, due to its vacancy. However, the high in cost and time suggest that further revisit of this method must be justify by the results obtained on my first trial. With the processed C-T result are detailly presented in journal entry 3 and 4, it is found that the variance of density upon the veneer does not concludes into the differentiation of visible features on the veneer. Hence after several method investigating the grey scale value on the veneer (grey scale represents local density, normalised within the image) such as manipulating the threshold all concludes into failure, the C-T method is disposed.

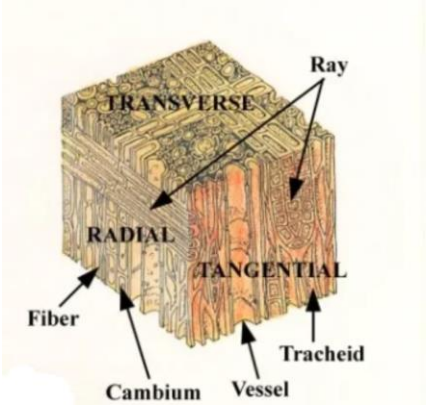

Figure 2.2.1 - 1: Method of Sectioning. [4]

Figure 2.2.1 - 1 shows the fibres, vessels, and rays, which represents radial, transverse, and tangential grain structures of a hard wood. It is desired that the microscopy investigation will provides the visualization of these features, so that further discussion with the team regarding which ones of these is problematic can be conducted. The microscopy results are mainly documented in journal entry 2, however due the large amount of image obtained, it is not possible to include all of them.

For instance, horizontal grain pattern in ***Figure 2.2.1 - 2(b)*** is the fibres which are not necessarily straight but wavy. The rays, displayed as vertical grainy structured patches in *Error!*

*Reference source not found.**(b)***, is scattered across the veneer and can be visualized by naked eyes by "lighter speckles patterns" as illustrated in ***Figure 2.2.1 - 2(a)***. Notably, it is later investigated that the speckles pattern appears in either light or dark dependent on the lighting direction and intensity.

(a) (b)

Figure 2.2.1 - 2: (a) The veneer piece put under microscope. (b) 2x Magnification of the area circled in red.

The pre-existing fracture regions of the veneer were placed under the microscope to identify any common features around that potentially results in the fractures. It is soon discovered that all fractures that are investigated fails around the presence of rays, suggesting a high likelihood of the change in grain direction being directly responsible for the fractures to occur. Figures in journal entry 2 illustrated the fractured surface magnified, evidencing the statement.

2.3 Designs

Scanning Module

By referencing the scanning method found in literature works, the design team concluded the options that can potentially be implemented into our system, as presented in journal entry 2. As shown in the journal, a weighted matrix is created based on the stakeholders' requirements.

The air-coupled ultrasound, with different setups, can measure the change in thickness, local density, presence of cracks, and young modulus of an object [5]. However, as the investigation from microscopy suggests, the cause of the stress concentration point is likely to be the rays' patches, which have diameter max out at roughly 1mm. Hence, a concern regarding the incapability of the ultrasound to achieve such resolution is raised and confirmed with literature results [2].

The contact transducer is commonly use in applications such as thickness gauging of thin materials and delaminating checks [6]. While the effect on the thickness is a potential issue, the grain direction is much more impactful than that. It is discovered that the veneer is stiffer to bend when the bend lines lie perpendicular to the fibres, and more prone to bend when parallel. As the stakeholders are only concern about the visual appearance of the veneer after their forming process, the crack or deformation under the surface is not to be taken account hence there will be no necessary for delaminating checks.

Hence, with above context and the result from the weighted matrix, it is suggested that a camera is the optimal choice and will be proceed for further determining the camera model.

It is evident in journal entry 4 that, the image obtained using a microscope under a 2 times magnification provides enough clarity on the rays' patches. Hence the detail of the figure is investigated and used as reference for me to carry out further investigation for the selection of the

camera model. Using conventional phone (Samsung's S23Ultra) camera with specifications of $12MP$, $1/2.55$" sensor, $1.4\mu m\ pixels$ and $f/2.2$ aperture lens, it was discovered that with 1.7x magnification and 3 cm from the object, it is sufficient to visualize the patches clearly, as illustrated in ***Figure 2.3 - 1***.

Figure 2.3 - 1: Image Captured using Conventional Camera.

Figure 2.3 - 2: Raspberry Pi HQ Camera Module.

With consideration of the integration of the camera module towards the raspberry pi eco-system (the data analysis team recommends a central computer for the whole system, and Raspberry Pi was decided as the optimal choice by Ven), the main scope of search for the camera module are those who can implement into the eco-system, as presented in journal entry 4. The process of selection is documented down using a mind map, as shown in ***Figure 2.3 - 3***, with the final, optimal decision chosen to be the Raspberry Pi HQ Camera Module. Note that this camera module requires an additional lens to operate. As presented in journal entry 4, it has met the requirements, with capability such as auto-focus and zoom capability.

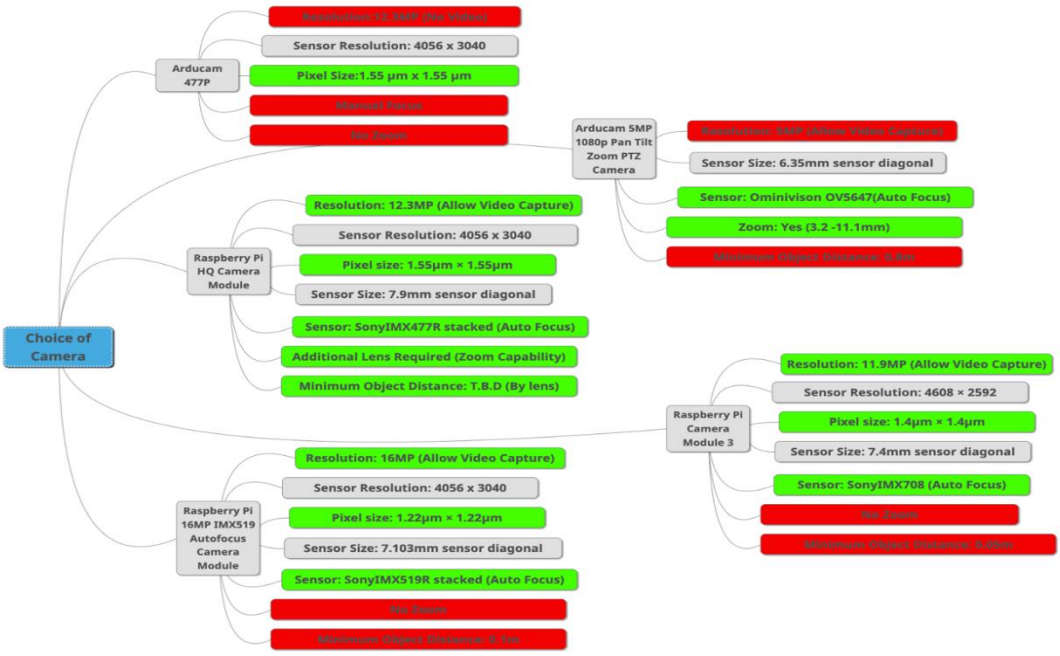

Figure 2.3 - 3: Mind – map for choice of camera.

The selection of lens located right after the camera on journal entry 4. The Pimoroni Microscope Lens demonstrated significant advantages, with optical zoom range from 0.12x to 1.8x and its' ability to focus under short distance to object ($2.4 - 36mm$) which is crucial since the reference figure used for obtaining the requirements are capture under microscope, with only approx. 3cm from the veneer. Unlike the other options, this lens will not limit the imaging resolution. Notably, it is more favourable to have a magnifying camera module (Zoom Capability) rather than physically shortening the distance between the object and the camera module itself. The inclusion of a physical device shortening the

distance suggest the necessity of a set of mechanism moving it in the vertically to the ground which introduce more variables and uncertainty towards the system and can potentially impact the overall system stability. Moreover, the movement of the scanning module vertically has a possibility in interfering with the lighting system, introducing risk of shadow casting onto the veneer.

With the Raspberry Pi camera module provides sufficient pixel resolutions, and the lens provides zoom capabilities and focus under low object distance, the scanning module is now fully capable in achieving our objective of capturing veneer features.

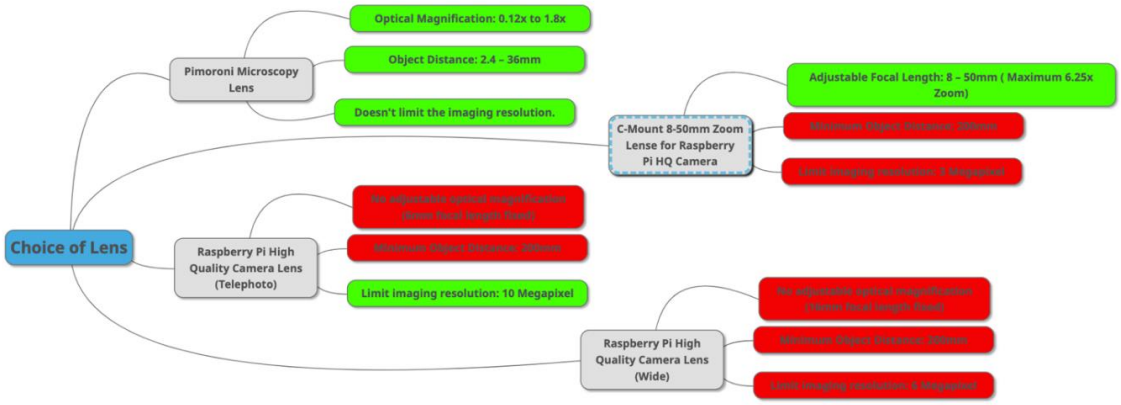

Figure 2.3 - 4: Mind-map for choice of lens.

It is discovered that the visual appearance of the veneer is sensitive to the lighting condition, varying the visual appearance significantly. Hence, a constant lighting setup must be designed and included for the image produced to be recognisable by the data analysis system. Starting off from the investigations conducted, to obtain the requirements for the lightning system.

(a) *(b)*

Figure 2.3 - 5: Appearance of the Veneer (a) Light shining perpendicular to the fibres' grain direction (from the top). (b) Light shining parallel to the fibres' grain direction (from the right).

Figure 2.3 - 5 illustrated the effect on altering the orientation of the light source. It was demonstrated that the lighting orientation affects the appearance of the ray patches and the fibres, which revealed that the lighting orientation (***Figure 2.3 - 6***) influences the appearance of both the ray patches and the fibres, causing one to appear darker than the other in certain orientation. The difference between this

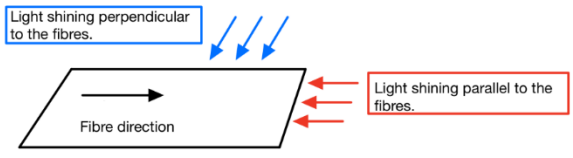

Figure 2.3 - 6: Orientation of Light.

veneer appearance under different lightning angle is minor, hence the only consideration for the angle is that it needs to be setup such that all the rays appear to be identical in colour under optical camera. Further investigation including the colour temperature are detailed in journal entry 4, the following depicted requirements obtained:

- Angled 45° for the light to cover the veneer based on the distance of the light horizontally and vertically from the veneer.
- 7cm from the veneer horizontally.
- 5cm above the veneer vertically.
- White light and diffuser (Colour temperature of 5600-6000K).
- Luminous intensity of 1000 lumens

The design of the component fitting the light source is hand towards another member in the wood structure team as they are relatively free at that time, and my responsibility here is to select a light source (strips) that fits well into the requirements.

Journal entry 5 detailed the light source selection, with the final selected strips that adhere closely to the specification will be the Ultra LED, ***Figure 2.3 - 7*** depicted the process of eliminating the choices. The criteria of "integration towards Raspberry Pi" not being prioritised in this matter, as the correct requirements is more important in visualising the features. Hence, although the Ultra LED cannot be integrated directly to the Raspberry Pi, it is still selected to be the best choice. Notably, another strip, WS2815B demonstrated high flexibility and tolerance towards future modifications. It is known by now that some veneers' visual appearances are sensitive towards the lightning condition. Considering other type of veneer that might requires a higher light intensity or different colour temperature, introducing a two light strips setup instead of one increase the inclusivity of our system. Thus, the ability of WS2815B to vary its colour temperature, and ease to integrate into the Raspberry Pi makes it the best choice to be implement into the system as a secondary strip.

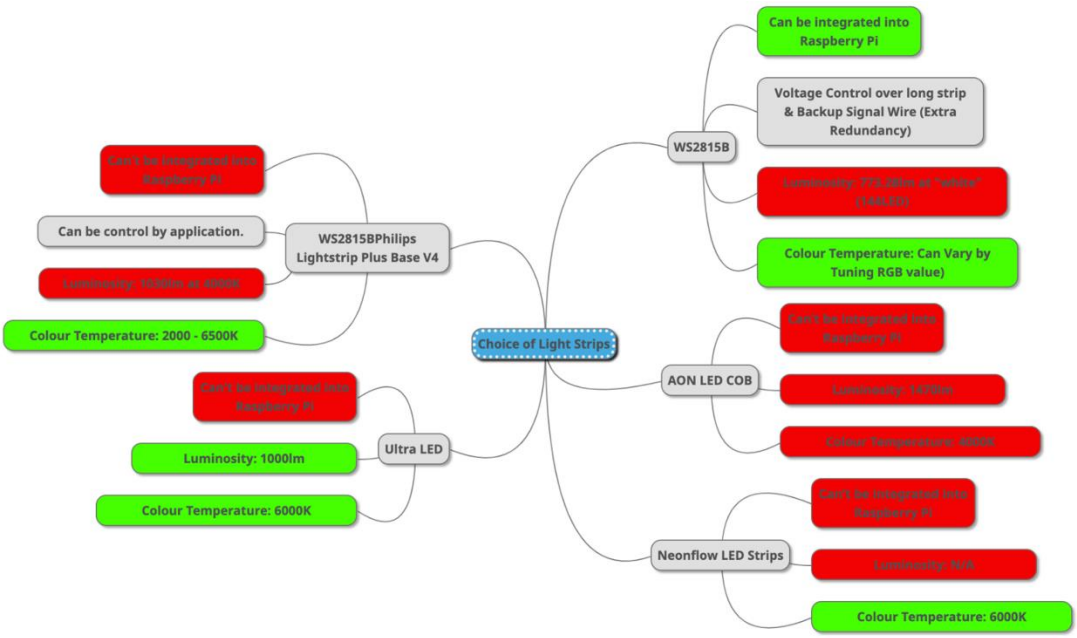

Figure 2.3 - 7: Mind – map of choice of light strips.

Coordinate Measuring Machine (CMM)

The choice of moving scanning module instead of a moving veneer platform (fixed scanning module) as detailed in entry 2 depicted the needs of us to have a CMM system for the module. After our discussion, I listed out the key points of each CMM method in Entry 4, with more detailed documentation (such as weighted matrix) completed by Ven. The final choice for our CMM is decided to be the gantry CMM due to its advantage in lower motor's load, simpler implementation, and higher stability (no resultant moment unlike cantilever or horizontal arm CMM). The size of the gantry CMM, needs to fulfill the maximum veneer size that are required by our stakeholders, which measures, 700mm x 130mm. After discussing with Ven, we decided to line up the longer side of the veneer as our primary axis (Figure 2.3 - 8) with the shorter side being our secondary axis. This is to reduce the load of the motor, and structural stress of the component by placing a lighter weight on top.

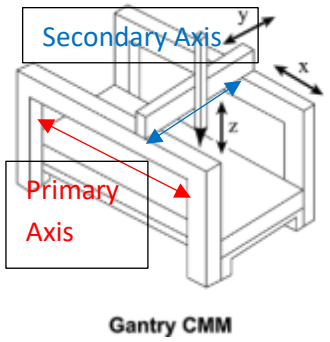

Figure 2.3 - 8: Example of Gantry CMM.

Criteria	Ball Screw
Power Efficiency	3
Effort and Frequency in Maintenance	2
Durability of System	4
Movement Speed	3
Weight	2
Cost	4
Versatility for Veneer Size	5
Integration within Raspberry Pi	5
Safety in Compliance to Industry Standards	3
Precision in Positioning	5
TOTAL	**142**

Table 2.3 - 1: Ball-screw weighting in the matrix.

The motion system that provides displacement of component on the CMM is a crucial part to be designed. Notably, the process of selecting the motion system starts earlier than the selection of type of CMM, as we are unclear about the concept of CMM until later stages. In journal entry 2, it is evident that the mind map, is paired with the weighted matrix to help us determine the motion system to implement. ***Table 2.3 - 1*** presented an example of the matrix, displaying the option with highest scoring, ball screw. While most of the criteria are self-explanatory, the "integration within Raspberry Pi", is to take note of, as some of the motion system requires additional motor to operate, hence integrations are between the motors and the Raspberry Pi. As most motors can be easily controlled using python, or C ++, it is most likely that they are fully capable of integrating into the Pi. Unlike the rack and pinion, the ball screw's resolution is not limited to the gear, while keeping clear from backlashes, which is a major disadvantage of the belt and pulley. It is also very versatile to the large veneer size (700mm length), which is required in this project while having great durability overtime, due to the implementation of ball bearings.

While there are linearized balls screw in the market, the length that we required it to be is rare, hence not common to be found. Also considering long axis needed to compensate with the length of the veneer, and additional tolerance length needed to ensure the clearance of other sub-system (for example lightning and camera system), a), a total length of around $1000mm$ in one of the axes depicted concerns regarding the moment acting on the ball screw. Hence, I decided to design our own linear guidance system for the ball-screw to also act as an additional structural support for the primary axis of our CMM.

As presented in journal entry 3, the selection of the linear guidance for the ball screw is detailed in a weighted matrix and the mind map. The v-slot aluminum extrusion, paring with a gantry plate in this context appears as the optimal solution, due to its' sufficient load capacity, minimal effort required in future maintenance. It is also beneficial that as an aluminum extrusion, the length can be customized and ordered easily, hence reducing waste material in this component, and keeping the component recyclable. The v-slot consist of a total of 4 rails, as exampled in ***Figure 2.3 - 9*** (and journal entry 3), the gantry plate only uses 2 of them, while keeping the top (relatively unused, but is somewhat blocked by the gantry) and bottom rails unattended, should any future designs or modification needed it.

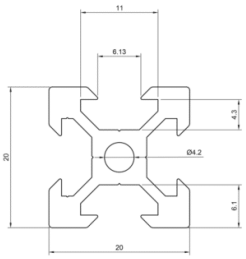

Figure 2.3 - 9: V-slot extrusion [online].

As for the secondary axis, it is much shorter hence will not requires additional structural support from the linear guidance system itself. A simple idea, that reference from existing product, as documented in journal entry 4, is developed and implemented instead. Compared to all the choices of linear guidance in entry 3, the 2 rods added on the side of the ball screw is enough in providing sufficient guidance, while make used of the existing hole available on the BK10 and BF10 (which are the end part of the ball-screw). While minimal material and effort is needed for this design, it has achieved its' objective in providing linear guidance while keeping wastage to the minimum, hence it is no doubt the optimal solution, presented also extra sustainability aspect to the project.

Moving towards the drive force for the ball screw, a motor type must be decided. The selection of it is completed by the Ven and I, with weighted matrix and mind map presented in journal entry 3. As a result, the stepper motor appears as triumph compared to other options, specifically in resolution, life expectancy, power efficiency. While there are other options, such as the servo motor, that performs similarly, the cost of reaching the same resolution and load capability is lower for stepper motor.

Proceeding into details, next will be the model of the stepper motor and the ball screw, as presented in journal entry 4. The primary axis on the CMM consist of 2 straight parts, one on each side, to support the secondary axis that lies on them. To eliminate any misalignment between the two parts when undergoing translation, it is better to include 2 motors, one per side to work synchronously. I then proceed in calculating the weight approximation for our system and obtained that the total weight is 90N. The torque required is bound by,

$$T = 0.5\ x\ Diameter\ x\ Weight \qquad \textit{Eqn. 1}$$

with the diameter here references the diameter of the ball screw. Hence, it is evident that the selection of the model for the stepper motor relies heavily on, with the model of ball screw. The common classification of ball screw includes the diameter, and the pitch, with common values of 12 -20mm, and 4 to 10mm respectively. A smaller diameter ball screw allows faster movement for the CMM and reduces the motor's load. A smaller pitch gives, higher precision, given a fixed step size from the motor. Hence, the best option will be to choose the one with smallest pitch and diameter, which is the SFU1204, representing diameter of 12mm, and pitch size of 4mm. It is also made fully metal, mainly steel and aluminium, thus all recyclables.

The minimum torque required hence can be calculated to be, 0.54Nm. Considering the torque curve goes down with rpm quite significantly, a torque two times higher than the minimum requirement would be reasonable to ensure smooth and fast movement. The step size of the stepper motor comes with either 0.9 or 1.8deg. The trade-off of a smaller step size, which gives higher precision, is the

significant reduction in torque and increment in cost. It is also calculated that when coupled with a ball screw model SFU1204, the difference of step size when translated into linear motion is minor, with 0.01 and 0.02mm per step only, respectively. Thus, as concluded in journal entry 4, a NEMA 23 stepper motor with torque range of 1.0Nm to 4.0Nm (if specifically, 23HE4S–2804S, the torque is 2.8Nm) is chosen as the optimal design option in this concern.

Subsequently, the coupling motion device/method needed to connect the ball screw with the stepper motor also needed to be decide. After my research online, the common methods are concluded to ***Figure 2.3 - 10.*** The following section in journal entry 4 detailed the reasoning behind the selection in this matter, with final decision going to the beam coupler, under the methods of shaft coupler.

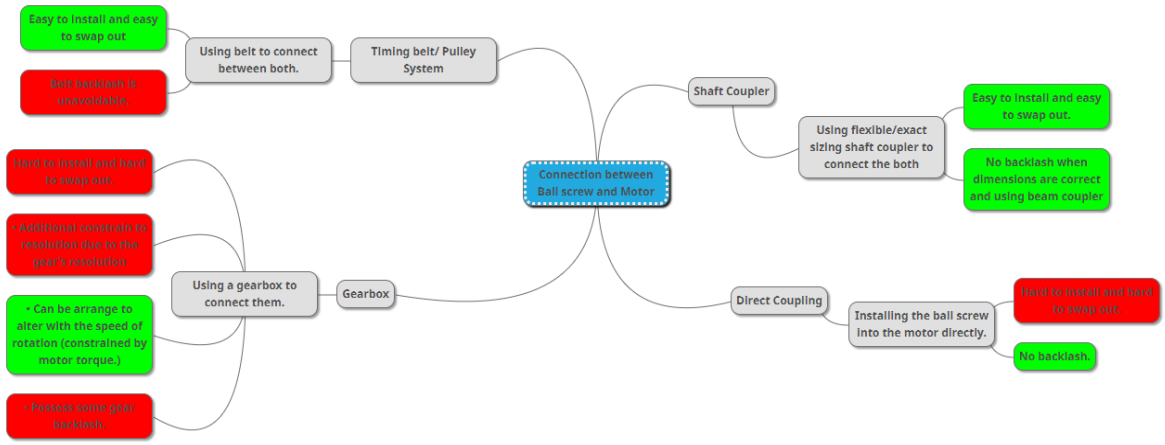

Figure 2.3 - 10: Mind map of connection between ball screw and motor.

Connectors

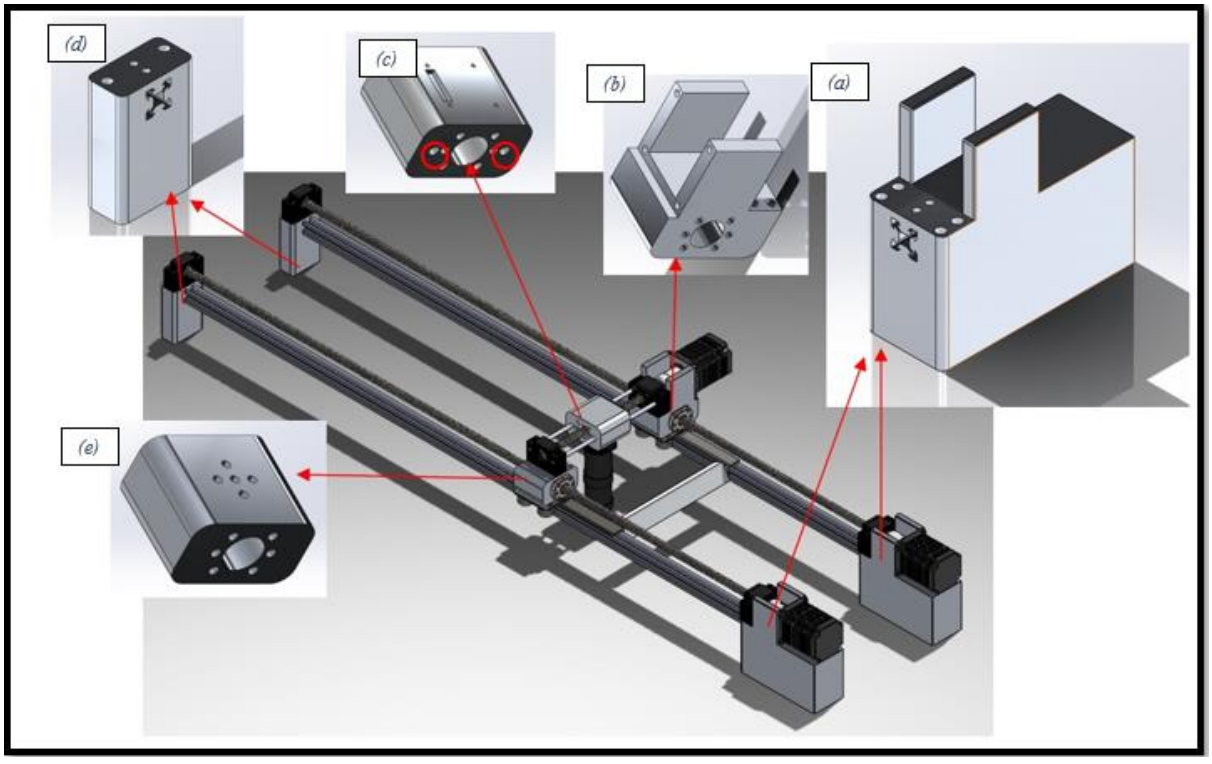

Figure 2.3 - 11: CAD Model of the CMM system including connector blocks and camera module.

To properly connect each sub-components together, some connectors need to be designed and implement into the system. ***Figure 2.3 - 11*** illustrated the designed connectors when implemented into the CMM system. Component (a) and (d) holds the v-slots in place, while providing a base for the ball screw's component, BK10 and BF10 respectively for the primary axis in the CMM. Additionally, component (a) also acts as the housing for the stepper motor, thus also the connection of ball screw and stepper motor through the beam coupler lies.

Component (b) and (e) primarily connects to the ball screws' nut, in the meantime providing linkage between the ball-screw and the gantry plate. Furthermore, the secondary axis's ball-screw's BF10 and BK10 also lies on these two components, with another stepper motor and beam coupler specifically lies on component (b) only. Component (c) is designed to hold the Raspberry Pi HQ camera module, while still connects back to the ball screw's nut on the secondary axis. It is also crucial to have an extra two holes on the sides of this component (circled in red on component (c) in ***Figure 2.3 - 11***), to fit in the two rods which will be acting as linear motion guidance specifically for the secondary axis.

The connectors designed in this section should all be manufactured using AA6061 aluminium alloy. As it is cheaper when compared to pure aluminium and lighter compared to steel. With ultimate tensile strength of 209 – 224MPa [10], it is providing sufficient strength to withstand the weight of the components as estimated above when selecting the motor.

Electronics

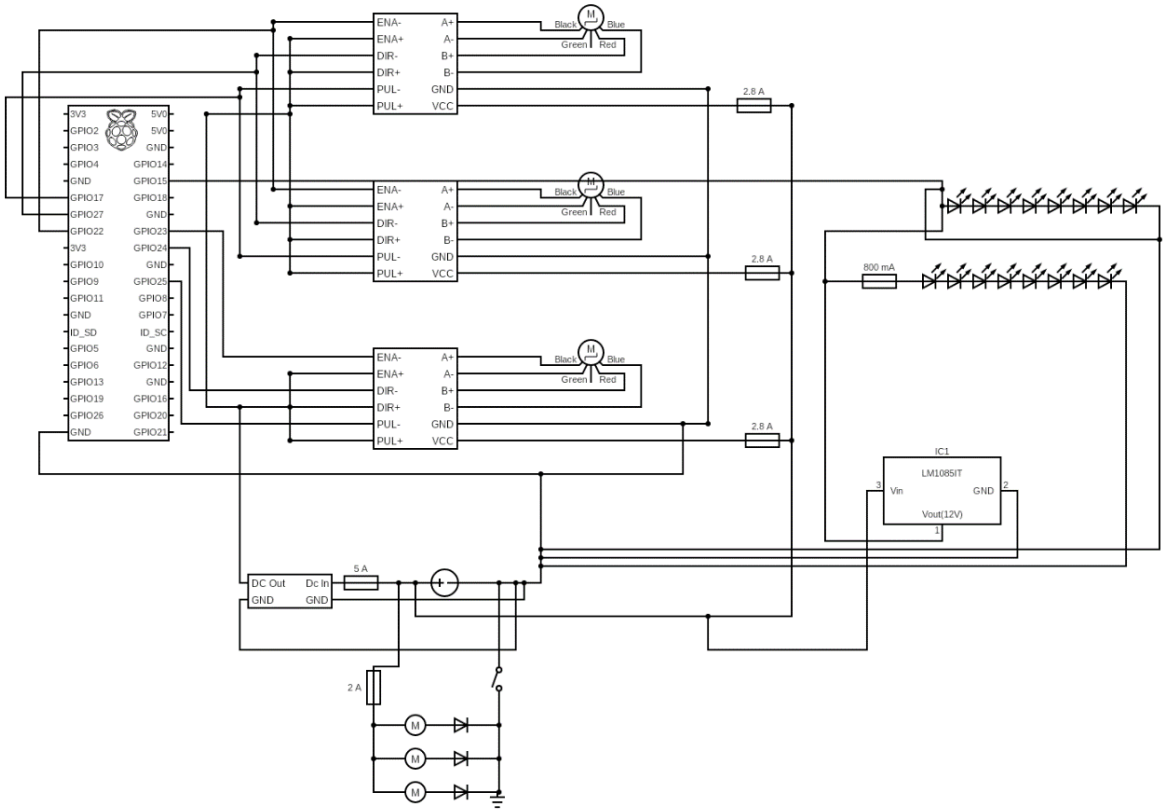

Figure 2.3 - 12: Circuit Diagram.

The circuit diagram constructed is as demonstrated in ***Figure 2.3 - 12***, with slight differ from the one in journal entry 5, which the vacuum system's circuit at the bottom in the diagram was not attached at the time. The main components that form the circuit includes, the Raspberry Pi 5, motor drivers, stepper motors, and the light strips. First, for the motor driver connection to the Raspberry Pi, I chosen the PNP connection, with positives output connected to controls input. The benefit of this connection is that it is more common among technicians, which suggest an easier understanding for the stakeholder's operator. As it is commonly not recommended to connect the ENA/DIR/PUL + ports to the Raspberry Pi 5V output [7], instead they are connected to 3.3V DC-DC converter which is protected by a 5A fuse and draws power from a DC supply. The negatives signals ports are hence connected back to GPIO ports on the Raspberry Pi, with 2 out of 3 drivers share the same GPIO in series connection. The ground and voltage in for the drivers needs to connect back to the power source, with 2.8A fuse in series for each driver and parallel connection between 3 drivers for equal voltage. As for the Ultra LED light strips, it should be connected to a 12V constant voltage regulator to ensure equal luminous intensity across the strips, with protection from an 800mA fuse. The WS2815B comes with 4 pins, the voltage in pin connects parallel with the Ultra LED to the 12V constant voltage regulator, the ground (GND) and backup input (BI) pins goes to the universal ground of the power source, and the data input (DI) goes to GPIO pin on the Raspberry pi. Note that since it is a light strip, only the first LED makes the above connections. From the 2nd onward LEDs on the WS2815B, the subsequent BI pins are naturally pre-connected to the previous DI pins. This is to prevent that the faulty of a single DI pins results in the lost in controls of subsequent LED, which is also the main difference of it being more superior that its ancestor models.

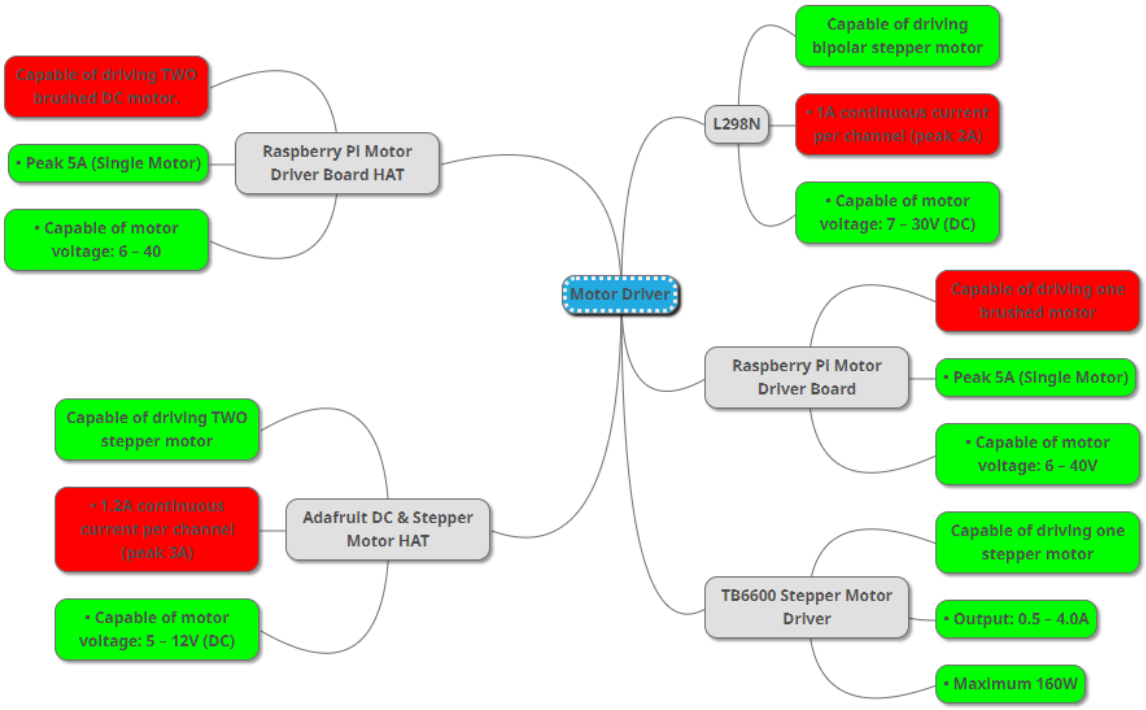

Figure 2.3 - 13: Mind map of the Motor Driver.

As mentioned on paragraph above, the stepper motor requires a logic driver for it to be functioning. The only restriction in selecting the driver would be a continuous 2.8A of current required by the NEMA 23 (23HE30-240S), and the compatibility of the driver towards a stepper motor. The

specifications of the driver found are listed out in journal entry 5 and concludes into the mind map ***Figure 2.3 - 13***.

Prototyping

A figure of the prototype constructed by Ven, and I is illustrated in journal entry 6. The prototype assembly includes the CMM and the camera module which is connected to a Raspberry Pi 5. The connectors as specifies in s***ection Connectors*** above used for this prototype, are manufactured by the 3D printer, using Polylactic Acid as materials, for low cost and time.

It is tested that the CMM movement are smooth, with the primary axis linear guidance, the v-slot and gantry plate fully operating in ensuring the linear motion of the movement. The secondary axis guidance, the 2 rods on the side is fits flawlessly, hence operating normally as anticipated.

The camera module is fully functioning however, the specification of the lens that claims its' object distance from 2.4mm to 36mm is false, with the actual minimum operating distance to be 50mm. With that, the setup must be raised up by some plywood, for the camera to focus. The lightning condition used in capturing the image is the exact same as the lightning specification, hence, some images are captured and feed to the data analysis team, for concept proofing of the code.

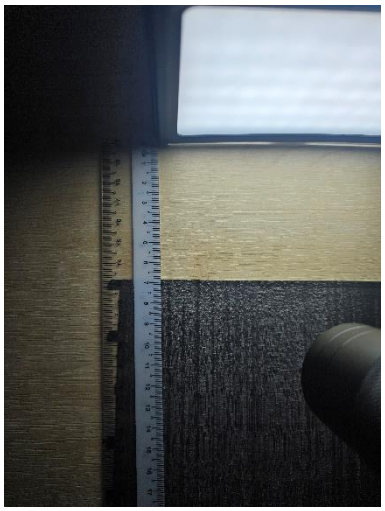

Figure 2.3 - 14: Distance from the veneer.

Final Design Proposal

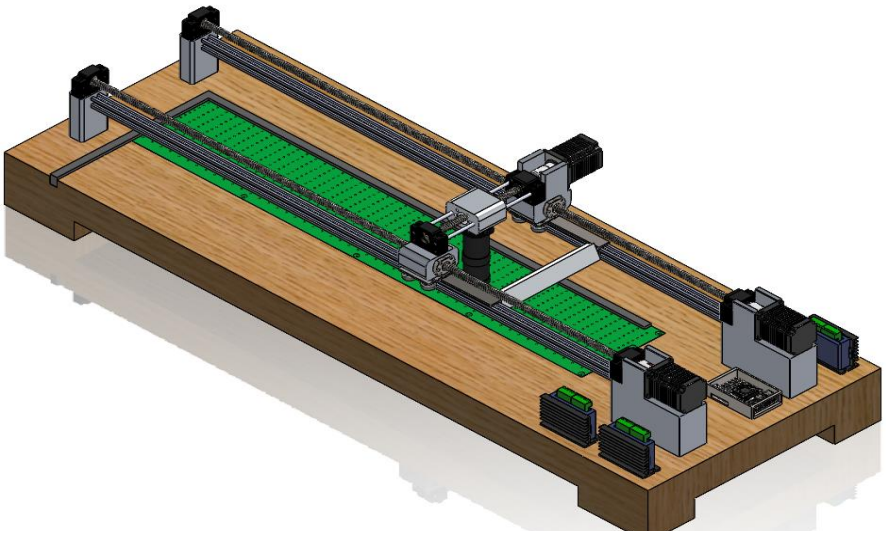

Figure 2.3 - 15: Final Design Proposal (Hardware).

The final design proposed by us in terms of hardware, is as illustrated as *Error! Reference source not found.Error! Reference source not found.*. The main sub-system includes the scanning module, which includes the camera, and the lightning system that is designed, or with its' model chosen. The gantry CMM, which is composed mainly by the ball screw and v-slot are responsible in transporting the scanning module, to ensure the ability of the system to conduct a full-sized scan for the veneer. Lastly, the base component is used for condemning the veneer on the surface, with a 90-degree alignment tool to fix the orientation of the veneer when placed on the base.

3. Key achievements

- Investigated the veneer using Microscope and C-T Scan.
    - Made an early assumption regarding the change in grain direction (rays' patches) results in stress concentration point.
- Designed the CMM as design team.
    - Chosen the Gantry CMM with details such as using V-slot as guidance, the model of the motor, etc.
- Investigated the lighting requirements for our system.
- Designed the Circuit Diagram.
- Prototyping and Concept Proofing for the CMM and camera module.

4. Critical review

Summary

The initial stage of the project is very challenging, as the veneer presented by the stakeholders have features that are not commonly found on literatures past work, hence the project was choked by trying to understand the visual appeared features and the characteristic associated with them. A method of modern machine learning, the convolutional neural network (CNN) was planned to be implemented during this stage, as the problem of identifying weak region seems to be complicated to resolve due to the complex visual appearances of the veneer. In the later stages when the information of the veneer is established, especially the relationship between the varying appearance and the lightning condition is confirmed, the need of complex machine learning model is redundant, hence a more straight-forward approach, the feature identification code instead was chosen. The hardware's main objectives are therefore the position translation of the camera to cover the entirety of the veneer, and ensuring the features that needs to be identify on the veneer can be captured by the camera throughout the operation. The final design proposal, consist of the combination of the software and the hardware, shows firm promises in delivering the stakeholders' requirements.

Pros

1. The project is well-structure and managed by correctly splitting into three teams, the wood structure, the design and manufacture and the data analysis. This allow us to develop the important aspect, hardware, and software simultaneously, as they are heavily co-related with each other, at the same time obtaining key pieces of information from the testing on the veneer.
2. The aims of the project, a data driven approach to solve the problem, is achieved.
3. 3 of out 4 of the objectives is achieved, with the only exception, the 68% detection rate, is falling short, as the focus on our assessment is solely on true positives. The human evaluation includes more false positives, hence possibly exhibits a wider range of error in detection accuracy.

Cons

1. The initial stage of the project, before the first main stakeholder meeting, is chaotic, due to the uncertainty induced by lack of information.
2. The communication of the main stakeholder is not as direct, due to legal issues.

Communication

The communication within the group throughout the stages is effective. Between the design team, the frequency of discussion being raised is very often, as the choices and options all needs to be talk over before deciding it to be the optimal in our context. Conversation between different teams plays a huge part in this project, as the information needed for each team to proceed on is often held and obtained

by the other team. Overall, the efficient and considerable amount of communication between the group is the key to piece the final design proposal together.

Innovation

1. The vacuum system designed to condemn the veneer is relatively portable when compared to literature works, as it only demands 3 conventional case fans to provide the pressure difference in the chamber.
2. The ball-screw, support and linearized by the v-slot are not available, or common in the market, with all the connectors designed specifically for this project.
3. The feature identification code that is developed to fulfil the objectives, are fully original.

Sustainability

The sustainability aspect in this project is fulfilled in most part throughout the design, as most part of the final design proposal's hardware made by recyclable materials. The success of this project suggests that wood veneer, can be considered more to be implemented in not only car interior, but also furniture, flooring, wallpaper etc, this will reduce the use of non-recyclable materials in decorative objects, contributing towards the sustainability for the world.

5. References

[1] Wang, J., Biernacki, J.M. & Lam, F. (2001) Nondestructive evaluation of veneer quality using acoustic wave measurements. *Wood Science and Technology*. 34 (6), 505–516. doi:10.1007/s002260000069.

[2] Fang, Y., Lin, L., Feng, H., Lu, Z. & Emms, G.W. (2017) Review of the use of air-coupled ultrasonic technologies for nondestructive testing of wood and wood products. *Computers and Electronics in Agriculture*. 137, 79–87. doi:10.1016/j.compag.2017.03.015.

[3] Purba , C. (2020) *MEASUREMENT OF BEECH VENEER DENSITY USING LASER SCATTERING METHOD*. In: 24 August 2020 Santiago.

[4] Hassani, N.J.M. (2018) Softwoods, Hardwoods, Sapwood, Pits, Fiber, Parenchyma, Tyloses, Resin Canal, Grain, Texture, Figure. *Forestrypedia*. https://forestrypedia.com/softwoods-hardwoods-sapwood-pits-fiber-parenchyma-tyloses-resin-canal-grain-texture-figure/.

[5] Anon (n.d.) *Air-coupled ultrasound: operating principle and applications - ZfP - BayernCollab*. https://collab.dvb.bayern/display/TUMzfp/Air-coupled+ultrasound%3A+operating+principle+and+applications#:~:text=Air%2Dcoupled%20ultrasound%20is%20a,and%20its%20fitness%20for%20purpose. [Accessed: 30 March 2024].

[6] Zhang, P. (2010) *Advanced industrial control technology*. 1st ed. Amsterdam Boston, William Andrew/Elsevier.

[7] Novellus (n.d.) *Raspberry Pi, Python, and a TB6600 Stepper Motor Driver*. Instructables. https://www.instructables.com/Raspberry-Pi-Python-and-a-TB6600-Stepper-Motor-Dri/ [Accessed: 2 April 2024].

[8] Anon (n.d.) *100X Industrial Microscope Lens, C/CS-Mount, Compatible with Raspberry Pi HQ Camera | 100X Microscope Lens for Pi*. https://www.waveshare.com/100x-microscope-lens-for-pi.htm.

[9] Anon (n.d.) *Pull out Torque Curve of 23HP22-2804S*. https://www.omc-stepperonline.com/download/23HP22-2804S_Torque_Curve.pdf.

[10] Ho, C. & Mohd Nor, M. (2021) Tensile behaviour and damage characteristic of recycled aluminium alloys AA6061 undergoing finite strain deformation. *Proceedings of the Institution of Mechanical Engineers, Part C: Journal of Mechanical Engineering Science*. 235 (12), 2276–2284. doi:10.1177/0954406220950349.